Supporting Information

Nomura et al. 10.1073/pnas.1200051109

SI Materials and Methods

Purification and Protein Incorporation into Liposomes. ***Sucrose method.*** A total of 2 mg of a lipid or a mixture of lipids dissolved in chloroform was dried under a stream of nitrogen. Distilled water (5 μL) was then added to prehydrate the lipids, followed 5 min later by 1 mL of 0.4 M sucrose. The solution was placed in the oven at 55 °C for 3 h, after which time, the appropriate volume of MscS and MscL was added to make a protein-to-lipid ratio of 1:1,000 (wt/wt) for both proteins.

D/R method. This method followed closely that described by Häse et al. (1). Lipids (2 mg) were dissolved in a glass test tube using $CHCl_3$. D/R buffer (1 mL) was added, and the solution sonicated for 15 min to form a cloudy liposome suspension. This was transferred into a 15-mL falcon tube, and a further 2 mL of D/R buffer was added. The desired quantity of MscL and/or MscS was then added and the solution was placed on a rotary wheel for 1 h. After this time, BioBeads (Bio-Rad) were added and the suspension mixed for a further 3 h. The solution was centrifuged at 250,000 × *g*, and the pellet was collected and spotted onto a microscope slide and dehydrated under vacuum overnight at 4 °C. The dried film was rehydrated with D/R buffer at 4 °C and subsequently used for experimentation.

Electrophysiology. Before recording the channel activity in liposome patches, an aliquot of liposomes (2–4 μL) was placed on the bottom of the experimental chamber containing the recording solution. Several minutes after adding the lipid, unilamellar blisters emerged from the collapsed liposomes, which were then used to create membrane patches in patch pipettes (Fig. S1) (2). Negative pressure (suction) recorded in millimeters of mercury was applied to patch pipettes using a syringe or High Speed Pressure Clamp-1 apparatus (HSPC-1; ALA Scientific Instruments) (3) and was monitored using a piezoelectric pressure transducer (Omega Engineering). We also tested the MscS and MscL response to linear ramps applied at different pressure rates to examine whether the rate of pressure application affects the TR (Fig. S2 and Table S2). Borosilicate glass pipettes (Drummond Scientific) were pulled using a Flaming/Brown pipette puller (P-87; Sutter Instruments). Electrodes with resistance of 2.5–4.9 MΩ (bubble number, 4.0–5.0) were used for the patch-clamp recording from inside-out spheroplast and liposome patches.

Patch Fluorescence Confocal Microscopy and Data Analysis. Fluorescence images from excised inside-out membrane patches, which consisted of azolectin (99.9%) and rhodamine-PE (0.1%) containing wild-type MscS and MscL, were observed using a Zeiss LSM 700 confocal microscope using a long working distance water immersion objective (63×; NA 1.15; Carl Zeiss) specially situated in a Faraday cage. The same electrophysiological recording solution was used as for the patch-clamp studies. A 555-nm laser line was used to excite the fluorophore labeled patches with emission detected using a long pass 560-nm filter. To visualize liposome patches the pipette tip was bent ~30° with a microforge (Narishige; MF-900) to become parallel to bottom face of the chamber.

To calculate membrane tension ratios, we used a variation of Laplace's law (4). Laplace's law states:

$$T = P(r/2)$$

where T is membrane tension, P is pressure, and r is the radius of the membrane curvature. From confocal images taken of the patch membrane, it was relatively simple to calculate the radius of the membrane patch under pressure and, thus, calculate the membrane tension (Fig. S1) (4, 5).

SI Data

Comparison Between the Activation Threshold and the Activation Midpoint in Determining the Activation Ratio (MscL/MscS). The channel activities were measured by the application of negative pressure through a patch pipette to the inside-out membrane patches by using HSPC-1 (*SI Materials and Methods*). Typical currents of wild-type MscS and MscL in *E. coli* giant spheroplasts and liposomal membranes are shown in Fig. 1 *A* and *B*, respectively. When an increasingly negative pressure was applied to the patch membrane, MscS opened first (Fig. 1 *A* and *B*, arrowhead). Further increases in the negative pressure opened MscL (Fig. 1 *A* and *B*, arrow). The dotted line and dashed line show the MR of MscS and MscL that were calculated by fitting a Boltzmann distribution function (Fig. 1 *A* and *B*). Negative pressure was applied until MscL channels were saturated. The TR was 2.01 ± 0.03 ($n = 6$) in spheroplasts and 2.70 ± 0.15 ($n = 7$) in liposomal membranes (Fig. 1*C* and Table S3). In contrast, the MR was 2.08 ± 0.04 ($n = 6$) in spheroplasts and 2.84 ± 0.18 ($n = 7$) in liposomal membranes, (Fig. 1*C* and Table S3). Although slightly larger than the TR, the MR did not differ significantly from it (Fig. 1*C*). The activation ratios in liposomal membranes were significantly higher than those in spheroplasts for both TR and MR (Fig. 1*C*).

The TR and the MR for MS channels can also be estimated by measuring tension instead of pressure using patch fluorescence confocal microscopy. A moderate suction was applied to the inside-out patch membrane until the membrane ruptured and MscS and MscL channel saturation was observed in liposome patches (Fig. 1*D*). Fig. 1*E* shows activation curves of MscS and MscL as measured with simultaneous confocal imaging of the patch pipette (Fig. 1*F*). All data points were fitted using a Boltzmann distribution. The midpoint of MscS activation was 6.2 ± 0.1 mN/m, whereas that of MscL was 12.0 ± 0.3 mN/m (Fig. 1*E*), which are higher than those previously reported for MscS (6) and MscL (7) reconstituted into liposomes. It should be mentioned, however, that previous measurements were obtained from patches in which the MscS and MscL channels were individually reconstituted and not coreconstituted. From the solid lines fitted to the Boltzmann distributions from four experiments, we calculated the mean values across the datasets for the MscL and MscS energies of activation to be 28.7 ± 8.1 and 22.3 ± 2.1 kT, respectively, where kT is a unit of energy used in molecular systems ($k = 1.38 \times 10^{-23}$ J/K is the Boltzmann constant and T is the absolute temperature in K). These values are in a very good agreement with the published data for both channels [32.4 ± 10.3 kT for MscL (8) and 24 ± 4 kT for MscS (9)]. The TR from our coreconstituted samples was 1.72 ± 0.04 ($n = 4$), whereas the MR was 1.86 ± 0.08 ($n = 4$) (Table S4). These ratios based on membrane tension measurements were not statistically different from each other. Overall, we have found no significant difference between measuring the TR compared with the MR.

Channel Activity of MscS and MscL. The channel activity of MscL and MscS coreconstituted into liposomes was examined using the patch-clamp recording from inside-out liposome patches. As previously reported (10) the coreconstituted channels opened at different applied pressure thresholds in patch pipettes. MscS channels opened at lower pressure thresholds than MscL channels. This is comparable to their behavior in native membrane

patches of *E. coli* giant spheroplasts (11, 12). The TR of MscL relative to MscS (MscL/MscS), defined as the ratio of the pressure applied to a patch pipette at which the first MscL and MscS channels opened in azolectin (100%) liposomes respectively was 2.29 ± 0.07 (n = 18) (Table S1).

To examine whether the difference of pressure application rate affects the TR (MscL/MscS), negative pressure was applied using the HSPC-1 apparatus (see *SI Materials and Methods*). Fig. S2*A* shows raw superimposed current traces with the negative pressure ramps applied at different pressure rates. As the pressure rate increased, the activation threshold for both MscS and MscL initially increased and finally reached a plateau, first for MscS and then for MscL (Fig. S2*B*) (Table S2). This could be a consequence of the adaptation that both MscL and MscS channels exhibit in excised membrane patches attributable to the mechanics of the lipid bilayer linking the channel adaptation in excised liposome patches to the relaxation of the inner monolayer, which is not in contact with the glass wall of the patch pipette (1, 13).

Moving of the Patch Membrane Does Not Affect the MscL/MscS Activation Threshold. Previous studies have reported that cell-attached patches flow continuously up into the patch pipette even in the absence of negative pressure (14, 15). Consequently, the surface area of the patch membrane is increasing due to this spontaneous movement. According to the Laplace's law the membrane surface tension is proportional to the pressure applied to the patch pipette and the radius of the membrane patch. Thus, the first opening of MscS and MscL will be observed at lower pressures as the membrane patch continues creeping up the pipette and the activation threshold of both channels will apparently decrease.

To ascertain whether an excised liposome patch creeps up the pipette, we used patch fluorescence confocal microscopy to monitor patch movement (Fig. S3*A*) and measured the time course of activation threshold of both MscS and MscL at 5, 15, and 30 min. The activation threshold of both MscS and MscL showed a significant time-dependent decrease (Fig. S3*B*). The rate of patch creeping was relatively fast until about 15 min and then slowed afterward, which corresponded to a trough in the activation threshold for both channels. Fig. S3*C* shows the time dependency of the MscL/MscS TR. Initially, the TR increased slightly after 5 min; however, no significant difference was observed throughout the experiments. These results provide further support for the previously reported applicability of Laplace's law to the activation of MS channels by membrane tension (4, 16).

Lytic Tension Breaking a Membrane Patch. We can exclude the possibility that cholesterol might have affected the geometry of liposome patches in our experiments because a change in curvature of the liposome patch cannot be detected by patch imaging, although local curvature has been indicated to influence MscL dynamics (17). Patch fluorescence confocal microscopy experiments on liposome patches with and without cholesterol confirmed that the patch geometry remained unchanged upon addition of 30% cholesterol, the highest cholesterol concentration used in our experiments (Fig. S4 *A* and *B*). In our experiments, we indicated that increasing the cholesterol content affects the thickness and stiffness of the liposome bilayer. We were curious as to how this might also affect the robustness of the membrane patch, so we determined the lytic tension of the liposome patches in response to increasing negative pressures using patch fluorescence confocal microscopy (Fig. S4 *A* and *B*). There were no significant differences in lytic tension between azolectin (99.9%)/rhodamine-PE (0.1%) and azolectin (69.9%)/cholesterol (30%)/rhodamine-PE (0.1%) membranes because the lytic tension for liposome patches without cholesterol was 22.1 ± 1.6 mN/m compared with 20.1 ± 1.7 mN/m for liposome patches with cholesterol (Fig. S4*C*). These lytic tensions correspond well with the values for lytic tensions reported in the literature (18). However, the lytic tension of azolectin (99.9%)/rhodamine-PE (0.1%) liposomes, which were reconstituted with wild-type MscS and MscL was significantly lower (Fig. S4*C*). The inclusion of the proteins was the likely cause for reducing the lytic tension threshold.

Orientation of MscS in Liposomal Membrane. It has been reported that MscS shows rectification at negative pipette potentials in inside-out excised membrane patches (6, 9, 19). We compared current to voltage relationship between MscS channels in giant spheroplast patches and those reconstituted into azolectin (100%) liposomes. Fig. S5 shows current–voltage (I-V) curves obtained under symmetrical ionic conditions [200 mM KCl, 40 mM $MgCl_2$, and 5 mM Hepes, pH 7.2 adjusted with KOH in both bath and pipette (Fig. S5, filled circles) in liposome experiments, and asymmetrical ionic conditions with the bath solution containing 250 mM KCl, 90 mM $MgCl_2$, and 5 mM Hepes, pH 7.2 adjusted with KOH (Fig. S5, open circles) in spheroplast experiments]. I-V curves obtained with both spheroplast and liposome patches showed rectification at negative pipette potential. The single channel current obtained from spheroplast patches was slightly higher than that of liposome patches at positive pipette potential, which is consistent with the difference of ion concentrations between the bath and the pipette solution. Therefore, these results indicate that MscS is oriented in the same right-side-out direction in both spheroplasts and liposomes. At present, we do not have a plausible explanation for it.

FLIM-FRET. We initially tried using the acceptor photobleach method to determine whether there was FRET between our samples. However, we noticed that following photobleaching there were false-positive results for donor only labeled samples due to either small sample movements, possibly as a result of laser tweezing from the strong photobleaching laser intensities; or by de-self-quenching of the donor fluorophores following photobleaching, whereby there is less self-quenching as a result of some of those fluorophores themselves being photobleached. As a result of this, we decided to use FLIM as a more certain indicator of FRET. To ensure that the azolectin did not exhibit any fluorescence lifetimes that were significantly shorter than the donor fluorophore AF488 and, thus, could be mistaken for clustering, we measured its autofluorescence lifetime. As can be seen in Fig. S6*A*, the FLIM of azolectin is considerably longer than that measured for AF488. Clustering of MscL with itself was reconfirmed using FLIM-FRET with regions of reduced fluorescence lifetime (blue) visible (Fig. S6*B*).

Before labeling the proteins with our fluorophores, we first ensured they were not clustered in solution by using fast protein liquid chromatography (FPLC) using an ÄKTA purifier (GE Healthcare/Pharmacia). This device separates proteins on the basis of size, with larger proteins, or larger clusters of proteins, exiting the column first. Simultaneously, this device will measure relative protein concentrations for each fraction by UV absorbance measurements. The trace in Fig. S6*C* displays an example of MscL protein being put through FPLC. The various fractions were also tested on SDS/PAGE electrophoresis gels to determine the size of the individual subunits to test whether they correspond to the MscL subunit size, which they do. As can clearly be seen from the FPLC trace, there seems to be some clustering of the purified MscL proteins in DDM buffer solution, and a larger peak that corresponds to a pentamer fraction as it exits the column at a similar period to other 80-kDa proteins. This large peak is followed by a smaller peak that perhaps is a MscL dimer fraction. For protein labeling, we chose to use the pentamer fraction only. FPLC and SDS/PAGE electrophoresis was also performed for MscS proteins.

For FLIM-FRET experiments, we reconstituted each fluorophore-labeled MscL and MscS sample into azolectin (100%) separately for 3 h before letting the samples mix together overnight.

The smaller MscL was incorporated at a ratio of 1 protein molecule per 10,000 lipids, whereas the larger MscS protein was incorporated at 1:28,000 molar ratio (giving a ratio of 1:100 wt/wt for each protein to lipid). The mixed reconstituted lipids were then ultracentrifuged to concentrate the lipid, and this lipid was then dehydrated overnight on a microscope coverglass before being rehydrated and fluorescence lifetime images of the fluorescence of the donor were collected.

1. Häse CC, Le Dain AC, Martinac B (1995) Purification and functional reconstitution of the recombinant large mechanosensitive ion channel (MscL) of Escherichia coli. *J Biol Chem* 270:18329–18334.
2. Delcour AH, Martinac B, Adler J, Kung C (1989) Modified reconstitution method used in patch-clamp studies of Escherichia coli ion channels. *Biophys J* 56:631–636.
3. Besch SR, Suchyna T, Sachs F (2002) High-speed pressure clamp. *Pflugers Arch* 445:161–166.
4. Sokabe M, Sachs F, Jing ZQ (1991) Quantitative video microscopy of patch clamped membranes stress, strain, capacitance, and stretch channel activation. *Biophys J* 59:722–728.
5. Sachs F (2010) Stretch-activated ion channels: What are they? *Physiology (Bethesda)* 25:50–56.
6. Sukharev S (2002) Purification of the small mechanosensitive channel of Escherichia coli (MscS): The subunit structure, conduction, and gating characteristics in liposomes. *Biophys J* 83:290–298.
7. Sukharev SI, Sigurdson WJ, Kung C, Sachs F (1999) Energetic and spatial parameters for gating of the bacterial large conductance mechanosensitive channel, MscL. *J Gen Physiol* 113:525–540.
8. Chiang CS, Anishkin A, Sukharev S (2004) Gating of the large mechanosensitive channel in situ: Estimation of the spatial scale of the transition from channel population responses. *Biophys J* 86:2846–2861.
9. Akitake B, Anishkin A, Sukharev S (2005) The "dashpot" mechanism of stretch-dependent gating in MscS. *J Gen Physiol* 125:143–154.
10. Battle AR, Petrov E, Pal P, Martinac B (2009) Rapid and improved reconstitution of bacterial mechanosensitive ion channel proteins MscS and MscL into liposomes using a modified sucrose method. *FEBS Lett* 583:407–412.
11. Sukharev SI, Martinac B, Arshavsky VY, Kung C (1993) Two types of mechanosensitive channels in the E. coli cell envelope: Solubilization and functional reconstitution. *Biophys J* 65:177–183.
12. Sukharev SI, Blount P, Martinac B, Kung C (1994) Functional reconstitution as an assay for biochemical isolation of channel proteins: Application to the molecular identification of a bacterial mechanosensitive channel. *Methods* 6:51–59.
13. Belyy V, Kamaraju K, Akitake B, Anishkin A, Sukharev S (2010) Adaptive behavior of bacterial mechanosensitive channels is coupled to membrane mechanics. *J Gen Physiol* 135:641–652.
14. Suchyna TM, Sachs F (2007) Mechanosensitive channel properties and membrane mechanics in mouse dystrophic myotubes. *J Physiol* 581:369–387.
15. Suchyna TM, Markin VS, Sachs F (2009) Biophysics and structure of the patch and the gigaseal. *Biophys J* 97:738–747.
16. Gustin MC, Zhou XL, Martinac B, Kung C (1988) A mechanosensitive ion channel in the yeast plasma membrane. *Science* 242:762–765.
17. Meyer GR, Gullingsrud J, Schulten K, Martinac B (2006) Molecular dynamics study of MscL interactions with a curved lipid bilayer. *Biophys J* 91:1630–1637.
18. Haswell Elizabeth S, Phillips R, Rees Douglas C (2011) Mechanosensitive channels: What can they do and how do they do it? *Structure* 19:1356–1369.
19. Martinac B, Buechner M, Delcour A, Adler J, Kung C (1987) Pressure-sensitive ion channel in Escherichia coli. *Proc Natl Acad Sci USA* 84:2297.

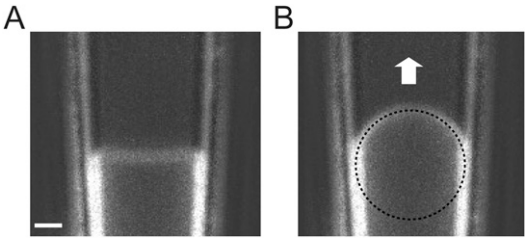

Fig. S1. Confocal microscopy image of a liposome membrane patch inside a patch pipette. Fluorescence image overlaid with transmission image in the absence (*A*) and presence (*B*) of negative pressure (arrow). A dotted circle is fitted to the patch membrane, and from the area of the circle, the radius can be calculated, which, along with the pressure measurements, can be used to calculate membrane tension. (Scale bar: 1 μm.)

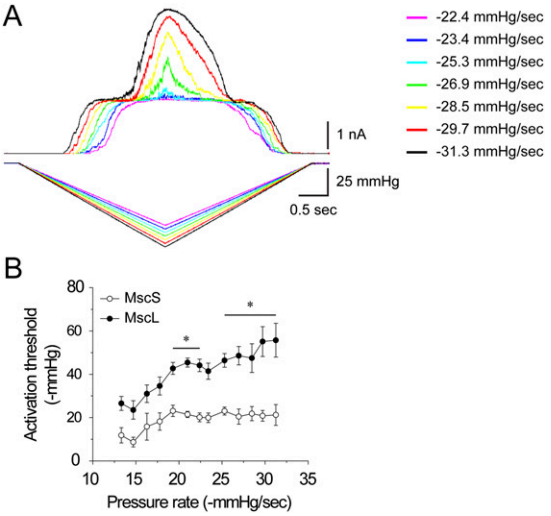

Fig. S2. MscS and MscL response to linear ramps applied at different pressure rates. (*A*) Representative superimposed current traces at different pressure rates ranging from −22.4 to −31.3 mmHg/s. (*B*) Activation threshold of MscS and MscL coreconstituted into azolectin (100%) liposomes at different pressure rates (mean ± SEM; $n = 3–9$). The asterisk indicates that the value is significantly different from pressure rate at −13.3 mmHg/s (*$P < 0.05$ by *t* test).

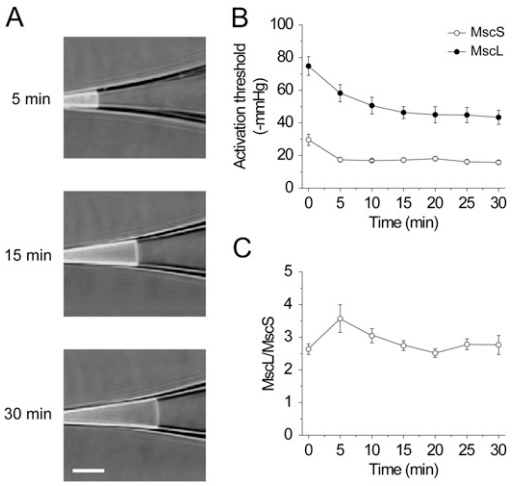

Fig. S3. The patch membrane creeps up the pipette interior causing the activation threshold of MscS and MscL to decrease in a time-dependent manner. (*A*) Movements of an excised inside-out liposome patch membrane at 5, 15, and 30 min, respectively, after a giga-ohm seal was obtained. The liposome patch membrane consisted of azolectin (99.9%) and rhodamine-PE (0.1%) fluorescent lipid. (Scale bar: 5 μm.) (*B*) Time course of activation threshold of MscS and MscL, respectively (mean ± SEM; $n = 6–7$). All values are significantly different from 0 min ($*P < 0.05$ by t test). (*C*) Time course of TR (mean ± SEM; $n = 6–7$).

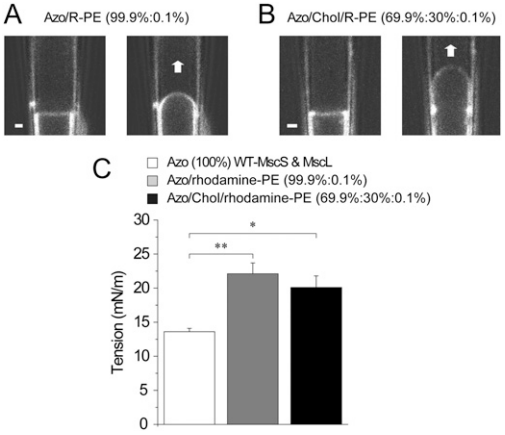

Fig. S4. Patch geometry and lytic tension of liposome patches without and with cholesterol. Patch geometry of liposome patches without (*A*) and with cholesterol (*B*) in the absence and presence of negative pressure (arrow). From the circumference of the circle, the radius was calculated. The radius was 2.69 and 2.34 μm without (azolectin 99.9%/rhodamine-PE 0.1%) and with cholesterol (azolectin 69.9%/cholesterol 30%/rhodamine-PE 0.1%), respectively. The membrane tension was 20.2 and 20.6 mN/m without and with cholesterol, respectively. (Scale bar: 1 μm.) (*C*) The lytic tension of each patch membrane is represented as mean ± SEM ($n = 5$). The asterisks indicate that the lytic tension of pure liposomes without or with cholesterol is significantly higher than that of azolectin (100%) liposomes reconstituted with MscS and MscL. $*P < 0.05$, $**P < 0.01$ by t test.

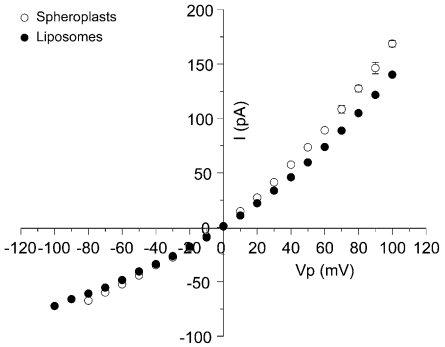

Fig. S5. I-V relationships of the wild-type MscS expressed in *E. coli* spheroplasts (MJF465) and reconstituted into azolectin (100%) liposomes. For experiments in liposomes, the pipette and bath solutions were the same, consisting of 200 mM KCl, 40 mM $MgCl_2$, and 5 mM Hepes with a pH 7.2 adjusted with KOH (●). In spheroplast experiments, the bath solution was different and contained 250 mM KCl, 90 mM $MgCl_2$, and 5 mM Hepes, pH 7.2 adjusted with KOH (○). V_p indicates the pipette potential. Data are shown as means ± SEM (n = 5–6).

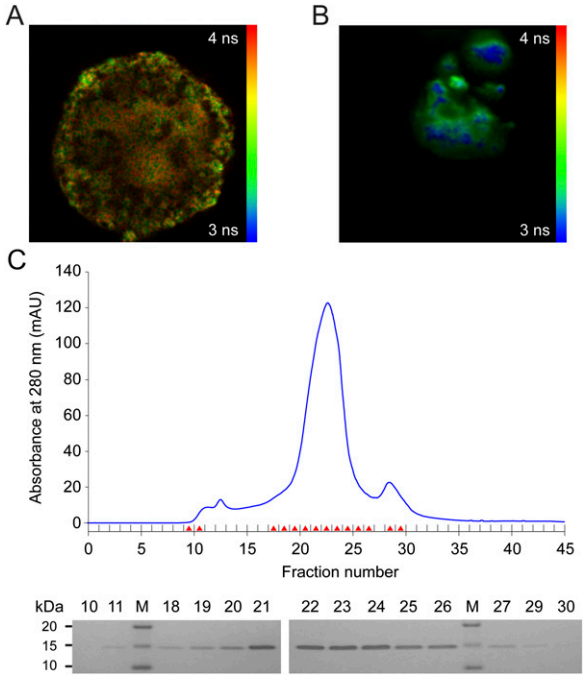

Fig. S6. FLIM-FRET. (*A*) Fluorescence lifetime image of unlabeled azolectin (100%). Lifetimes are typically longer than for AF488-labeled proteins. (*B*) FLIM image of azolectin (100%) sample containing separate populations of MscL M42C mutant proteins labeled with AF488 and another with AF568. Lifetimes are measured for the donor fluorophore (AF488) only. Regions colored blue show areas where fluorescence lifetimes are shorter as a result of FRET attributable to the close proximity of the MscL protein populations in the lipid, indicating clustering. As would be expected in situations where clustering occurs FRET is not exhibited uniformly in all regions of the lipid. (*C*) Fast protein liquid chromatography (FPLC) of MscL proteins with accompanying SDS/PAGE gel electrophoresis gels. Red arrowhead shows the fraction that corresponds to the lane number of SDS/PAGE. M indicates molecular mass marker.

Table S1. Activation threshold and threshold activation ratio of the coreconstituted MscS and MscL channels in liposome patches made of different lipid composition

	Activation threshold (mmHg)		Threshold activation ratio (MscL/MscS)	*n*
	MscS	MscL		
AW737 (WT) spheroplasts	−107.1 ± 7.57	−181.56 ± 11.96	1.70 ± 0.02	10
Azolectin (100%)	−18.23 ± 1.38	−41.23 ± 3.59	2.29 ± 0.07	18
Azolectin:cholesterol (95%:5%)	−32.08 ± 8.62	−54.19 ± 14.29	1.75 ± 0.07	9
Azolectin:cholesterol (90%:10%)	−28.49 ± 3.14	−42.25 ± 4.17	1.51 ± 0.05	10
Azolectin:cholesterol (80%:20%)	−42.33 ± 5.10	−58.64 ± 6.62	1.42 ± 0.04	15
Azolectin:cholesterol (70%:30%)	−40.76 ± 4.86	−52.15 ± 5.47	1.31 ± 0.04	13
PE18:PC18 (70%:30%)	−19.75 ± 2.08	−33.38 ± 4.42	1.67 ± 0.08	8
PE16:PC16 (70%:30%)	−17.72 ± 4.32	−24.47 ± 5.65	1.39 ± 0.11	7

The results obtained from the MscS and MscL channels coreconstituted into liposomes. The results from the channels recorded in the native membrane patches of giant *E. coli* spheroplasts (AW737 WT) are given for comparison. They correspond well to the previously reported results (1, 2). Negative hydrostatic pressure ramp was applied to patch pipettes by hand using a syringe. *n* indicates the number of different patches tested. All values represent means ± SEM.

1. Yoshimura K, et al. (1999) Hydrophilicity of a single residue within MscL correlates with increased channel mechanosensitivity. *Biophys J* 77:1960–1972.
2. Folgering JH, et al. (2005) Engineering covalent oligomers of the mechanosensitive channel of large conductance from Escherichia coli with native conductance and gating characteristics. *Protein Sci* 14:2947–2954.

Table S2. Summary of the results of MscS and MscL mechanosensitivity obtained at different pressure rates using HSPC-1

Pressure rate (mmHg/s)	Activation threshold (mmHg)		Threshold activation ratio (MscL/MscS)	*n*
	MscS	MscL		
−13.31	−11.78 ± 3.51	−26.51 ± 3.23	2.72 ± 0.57	4
−14.70	−8.66 ± 2.24	−23.48 ± 4.26	2.88 ± 0.34	3
−16.27	−15.76 ± 6.21	−30.97 ± 4.05	2.36 ± 0.50	3
−17.76	−18.15 ± 3.99	−34.55 ± 4.17	2.14 ± 0.28	5
−19.30	−23.06 ± 2.60	−42.68 ± 2.74*	2.04 ± 0.25	9
−21.00	−21.41 ± 1.41	−45.39 ± 2.09*	2.15 ± 0.11	7
−22.40	−20.09 ± 2.01	−44.07 ± 2.88*	2.31 ± 0.20	8
−23.40	−19.88 ± 2.18	−41.37 ± 3.75	2.15 ± 0.13	7
−25.30	−22.96 ± 1.83	−46.36 ± 3.15*	2.03 ± 0.06	7
−26.95	−20.41 ± 3.49	−48.55 ± 4.26*	2.53 ± 0.21	6
−28.47	−21.78 ± 3.27	−47.42 ± 6.63*	2.21 ± 0.15	6
−29.72	−20.79 ± 2.49	−55.06 ± 6.90*	2.69 ± 0.30	4
−31.25	−21.18 ± 4.79	−55.68 ± 7.81*	2.81 ± 0.29	4

n is the total number of recordings. The asterisk indicates that the value is significantly different from pressure rate at -13.31 mmHg/s (*$P < 0.05$ by *t* test). Data are shown as means ± SEM.

Table S3. Comparison of TR and MR for MscS and MscL recorded in both giant spheroplasts and liposomes

	Spheroplasts (AW737)	*n*	Liposomes (azolectin 100%)	*n*
MscL/MscS				
TR	2.01 ± 0.03	6	2.70 ± 0.15*	7
MR	2.08 ± 0.04	6	2.84 ± 0.18†	7
No. of channels				
MscS	70.8 ± 18.2	6	12.1 ± 2.7	7
MscL	26.4 ± 5.0	6	28.5 ± 4.3	7

All recordings were obtained using HSPC-1 at the pressure rate of −48 mmHg/s and −99 mmHg/s for liposomes and giant spheroplasts, respectively. *n* is the total number of recordings. The asterisk and dagger indicate that the value is significantly different from spheroplasts (*$P < 0.01$; †$P < 0.05$; by *t* test). Each value represents mean ± SEM.

Table S4. Comparison of threshold, midpoint, TR, and MR calculated from negative pressure and corresponding membrane tension applied to MscL and MscS coreconstituted into liposomes

	Pressure (mmHg)	Tension (mN/m)
MscL/MscS		
TR	2.00 ± 0.12	1.72 ± 0.04
MR	2.05 ± 0.07	1.86 ± 0.08
MscS		
Threshold	−49.35 ± 3.99	5.38 ± 0.17
Midpoint	−61.34 ± 3.22*	6.49 ± 0.10†
MscL		
Threshold	−98.15 ± 7.19	9.27 ± 0.15
Midpoint	−126.37 ± 9.26	12.06 ± 0.30†

The negative pressure was applied to patch pipettes by hand using a syringe. The asterisk and dagger indicate that the value is significantly different from threshold (*$P < 0.05$; †$P < 0.01$ by t test). Each value is represented as mean ± SEM ($n = 4$).